JPE 5-4-5

Simultaneous Estimation of Rotor Speed and Rotor Resistance of an Induction Motor Using Variable Rotor Flux

Zhen-Guo Lee[*] and Seok-Kwon Jeong[†]

[*]Department of Mechatronics, Graduate School, Pukyong National University, Busan, Korea
[†]Division of Mechanical Engineering, Pukyong National University, Busan, Korea

ABSTRACT

In this paper, a new speed sensorless induction motor scheme which can estimate rotor speed and rotor resistance simultaneously is presented. The rotor flux with a low frequency sinusoidal waveform is used to conduct on-line simultaneous estimation of the rotor speed and rotor resistance. Hence the proposed sensorless control method is robust to rotor resistance variations. Also, the control scheme has no current minor loop to determine voltage references. It contributes to good control performance at low speeds. Some simulation results supported by experiments are given to show the effectiveness of this method.

Keywords: Induction motor, Feedforward torque control, Speed sensorless control, Variable rotor flux, Simultaneous estimation, Speed estimation, Rotor resistance estimation, Robust control

1. Introduction

A number of sensorless induction motor drives have been developed in the past [1-5]. However, the performance of these sensorless drives is not sufficient when compared to the sensored ones. A major drawback of these drives is due to the difficulty of control at low stator frequencies. During this region of operation, the signal-to-noise ratio of the stator current is decreased significantly and the effect of the stator resistance voltage drop is not negligible. Another difficulty is to ensure the robustness of the drives against motor parameter variations, especially rotor resistance. Also, it is well known that simultaneous

estimation of speed and rotor resistance is hardly obtained in the vector control induction motor drives with constant rotor flux [5].

To solve these problems, we suggest a novel speed sensorless scheme based on a feedforward torque control technique[6]. The control scheme has some different features compared with the classical vector controls. First, the rotor flux is given as a sinusoidal waveform in the d,q reference frame without affecting the torque control performance. It is possible to estimate on-line both speed and rotor resistance using the rotor flux. Second, it does not have any current feedback loops. Thus, we do not need to consider any phase compensations due to the delay between stator voltages and stator currents. Since control voltage can be determined using this feedforward technique, we can exclude complicated processes in order to design PI gains in current regulators. Third, the

electromagnetic torque is controlled rapidly and independently of the rotor flux without inducing any spike current. Since we do not inject any high frequency signals to estimate the rotor resistance, we expect less current ripples and we do not need to design a high band-pass filter to reject them. Hence, we can reduce the burden of hardware to inject high frequency signals and also software to detect these high frequency signals.

In this paper, the feedforward type torque control is first described in detail using the machine equivalent circuit equations. Then, the estimation equations for rotor speed and rotor resistance are derived from stator currents in the d, q reference frame. After that, the speed sensorless scheme based on the feedforward torque control is described. Finally, through several simulation results using a PWM voltage-source inverter and experiments based on a DSP control system, the validity of the proposed method is verified.

2. Simultaneous Estimation of Rotor Speed and Rotor Resistance

2.1 The feedforward torque control

Fig. 1 shows the schematic diagram of the feedforward torque control. The most important feature of this method is that the voltage reference does not depend on any feedback stator currents.
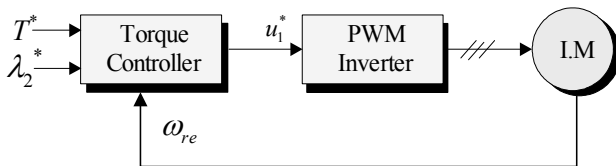

Fig. 1   Feedforward torque control scheme.

The voltage command which can get quick torque response is derived from motor circuit equations like (1). We use torque reference, rotor flux reference, speed information, and motor parameters to determine the voltage reference [6].

$$u_1^* = \left\{ \left(a_{1d}\lambda_2^* + a_{2d}\,p\lambda_2^* + a_{3d}\,p^2\lambda_2^* - a_{4d}\omega_{re}\frac{T^*}{\lambda_2^*} - a_{5d}\frac{T^{*2}}{\lambda_2^{*3}} \right) \right.$$

$$\left. + j\left(a_{1q}\omega_{re}\lambda_2^* + a_{2q}\omega_{re}\,p\lambda_2^* + a_{3q}\frac{T^*}{\lambda_2^*} + a_{4q}\frac{pT^*}{\lambda_2^*} \right) \right\} e^{j\omega_0 t} \quad (1)$$

$$\omega_0 = \omega_{re} + \frac{R_2 T^*}{P\lambda_2^{*2}} \quad (2)$$

where,

$$a_{1d} = \frac{R_1}{M} \qquad a_{2d} = \frac{L_1 R_2 + L_2 R_1}{MR_2} \qquad a_{3d} = \frac{\sigma^2}{MR_2}$$

$$a_{4d} = \frac{\sigma^2}{PM} \qquad a_{5d} = \frac{\sigma^2 R_2}{P^2 M} \qquad a_{1q} = \frac{L_1}{M}$$

$$a_{2q} = \frac{\sigma^2}{MR_2} \qquad a_{3q} = \frac{L_1 R_2 + L_2 R_1}{PM} \qquad a_{4q} = \frac{\sigma^2}{PM}$$

$$\sigma^2 = L_1 L_2 - M^2$$

Also, R_i, L_i ($i=1,2$: stator and rotor), M, P are the resistances, inductances, mutual inductance, and pole pair number. The notation '*' means reference value and p indicates differential operator ($= d/dt$). T means torque, λ_2 is rotor flux, and ω_{re} represents electrical angular velocity.

The stator current and rotor current can be controlled as (3-a) and (3-b) when we give the voltage command (1) and (2) to the motor model as reference[6].

$$\hat{i}_1 = \left\{ \left(\frac{\lambda_2^*}{M} + \frac{L_2}{MR_2}\,p\lambda_2^* \right) + j\frac{L_2 T^*}{PM\lambda_2^*} \right\} e^{j\omega_0 t} \quad (3\text{-a})$$

$$\hat{i}_2 = \left(\frac{p\lambda_2^*}{M} - j\frac{T^*}{P\lambda_2^*} \right) e^{j\omega_0 t} \quad (3\text{-b})$$

Where, notation 'Λ' means theoretical value from the motor reference model to distinguish the ideal value from the real value detected directly on motor.

It is noticed here that the currents have no transient terms about time t. Therefore, it is obvious that we can control the instantaneous electrical torque as a transient-less state with very quick torque response if we, theoretically, use the proposed voltage command (1).

2.2 Estimation of the rotor speed

Fig. 2 shows the speed estimation mechanism using the MRAC (Model Reference Adaptive Control). The theoretical q-axis current (4), output of the reference
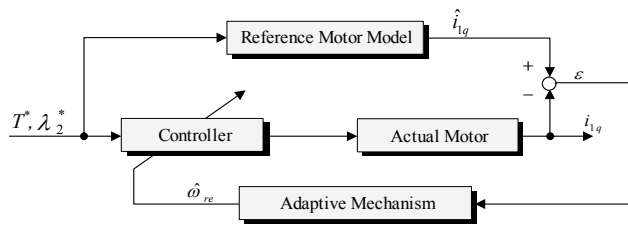
Fig. 2 Speed estimation mechanism using MRAC

motor model in Fig. 2, can be obtained from (3-a). Using this ideal current $\hat{i}_{1q}$ and detected current i_{1q} from the real motor, the rotor speed which we want to estimate can be formulated as (5).

$$\hat{i}_{1q} = \frac{L_2 T^*}{PM\lambda_2^*} \tag{4}$$

$$\hat{\omega}_{re} = K_{pT}\lambda_2^*\left(\hat{i}_{1q} - i_{1q}\right) + K_{iT}\int \lambda_2^*\left(\hat{i}_{1q} - i_{1q}\right)dt \tag{5}$$

Where, K_{pT} and K_{iT} represent proportional gain and integral gain respectively. The torque controller gives the voltage reference (1) as a control input to the actual motorin Fig. 2. It is noted here again that (5) does not have R_2.

2.3 The variable rotor flux with sinusoidal waveform

Fig. 3 shows an equivalent circuit of induction motors when the part of q-axis of rotor flux is supposed at zero.
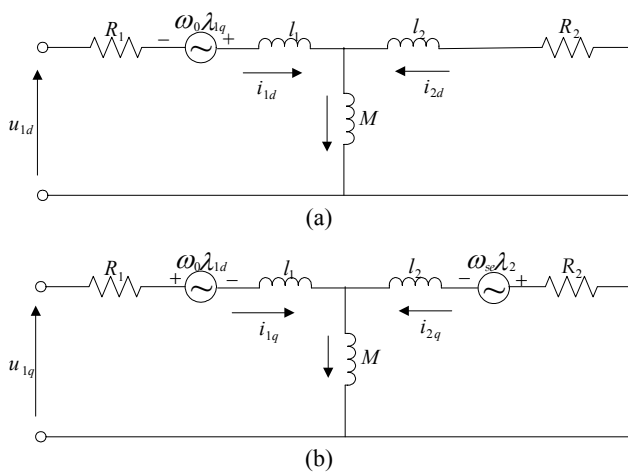

(a)

(b)

Fig. 3 Equivalent circuit in a synchronous reference frame; (a) rotor flux axis, (b) torque axis.

Where, u_{1d} and u_{1q} represent a component of d and q-axis of source voltage individually. Also, λ_{1d}, λ_{1q} and λ_2 mean d and q-axis components of stator flux, and rotor flux. ω_{se} indicates slip angular frequency.

The stator currents can be derived as follows in d, q reference frame;

$$i_{1d} = \frac{1}{M}\lambda_2 + \frac{L_2}{M}\frac{1}{R_2}p\lambda_2 \tag{6-a}$$

$$i_{1q} = \frac{L_2}{M}\frac{1}{R_2}\omega_{se}\lambda_2 \tag{6-b}$$

where,
$$\lambda_{2d} = Mi_{1d} + L_2 i_{2d} = \lambda_2$$
$$\lambda_{2q} = Mi_{1q} + L_2 i_{2q} = 0$$

If we give the rotor flux as a conventional constant value, we know that we can not get rotor resistance information from (6-a). Furthermore, it is noticed that the rotor resistance and slip frequency can not be obtained simultaneously from (6-b). However, it is very clear that if we give the rotor flux as a sinusoidal waveform properly, we can estimate the rotor speed and rotor resistance simultaneously from these (6-a) and (6-b).

If we give the rotor flux as a sinusoidal waveform (7), then the rotor resistance can be derived as (8).

$$\lambda_2^* = \lambda_R(1 + A\sin Bt) \tag{7}$$

$$\hat{R}_2 = \frac{L_2 B^2 \lambda_R}{Mpi_{1d} - p\lambda_2^* + \frac{L_2 B^2}{\hat{R}_2}\lambda_2^*} \tag{8}$$

As shown in (8), the rotor resistance can be estimated simply without calculating troublesome trigonometric functions and complicated integral computations. Also, the estimation of the rotor resistance can be conducted simultaneously with speed estimation (5).

2.4 Speed sensorless control system

Fig. 4 shows a speed sensorless control system based on (5) and (8). It consists of four major parts such as speed controller, torque controller, rotor resistance estimator,

and rotor speed estimator. The speed and rotor flux are given to the speed controller as a command. The speed estimator uses rotor flux, torque, detected stator currents, and motor parameters. Also, the rotor resistance estimator uses estimated speed, motor parameters, and detected motor stator currents. In this figure, the torque controller, the speed estimator and the rotor resistance estimator are used in equation (1), (5), and (8) individually.
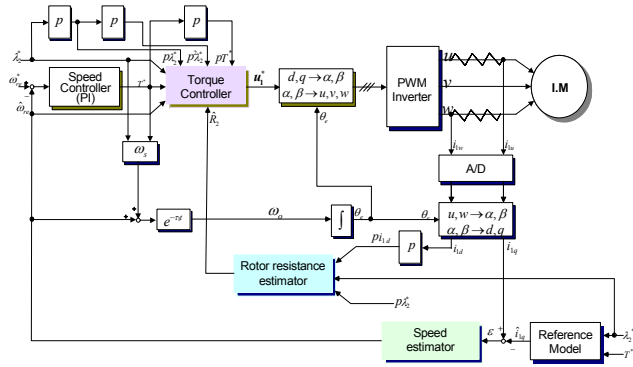

Fig. 4   Speed sensorless control system

3. Numerical Simulation

To verify the proposed sensorless control scheme, simulations are performed using the PWM voltage-source inverter and an I.M whose parameters are listed in Table 1. The carrier frequency is set at 3 kHz and the sampling times for speed calculation and current integration of mathematical I.M model are set at 1 ms, and 1 μs respectively. At first, the feedforward torque control performances are investigated based on Fig. 4.

Table 1   Rated values and motor parameters.

P_R	2.2 [kW]	P	2
u_R	220/380[V]	i_R	9.2/5.3[A]
R_1	2.54[Ω]	R_2	0.43[Ω]
L_1	169.11[mH]	L_2	169.11[mH]
M	163.25[mH]	J	0.003[$Nm \cdot s^2 / rad$]

As we focused on torque control performance, we excluded the speed controller, rotor resistance estimator, and rotor speed estimator in Fig. 4. The actual rotor speed was calculated by using information on currents and motor
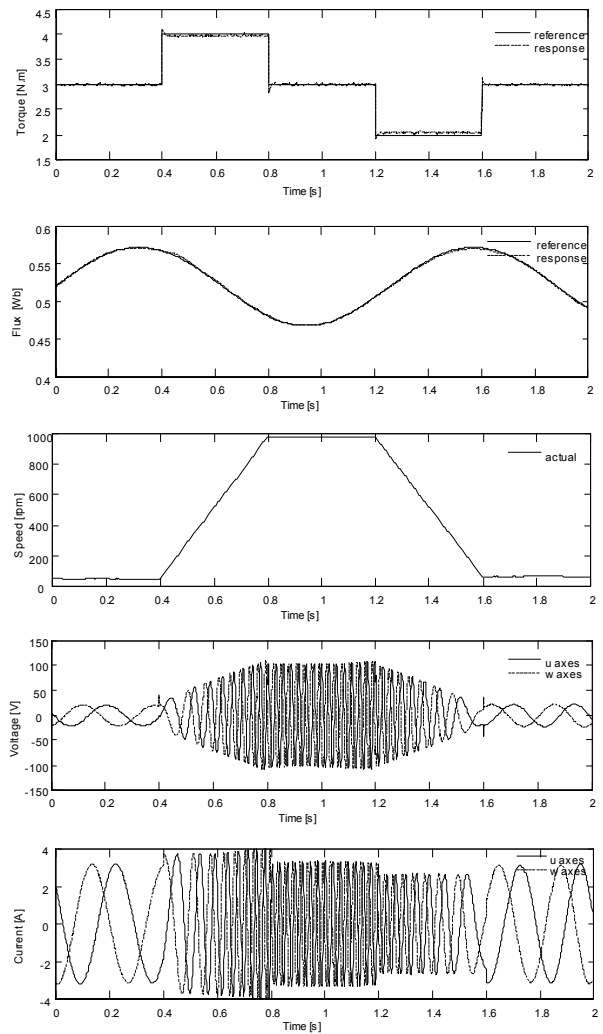

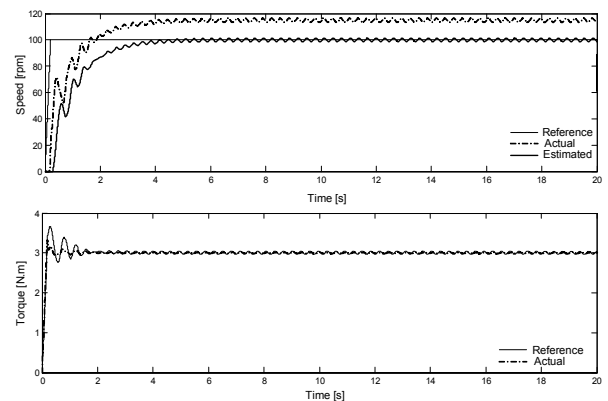Fig. 5   Torque response according to stepwise command

Fig. 6   The effect of estimation error of the rotor resistance

inertia in this simulation. Also, we supposed that the rotor resistance had real value and it was not changed.
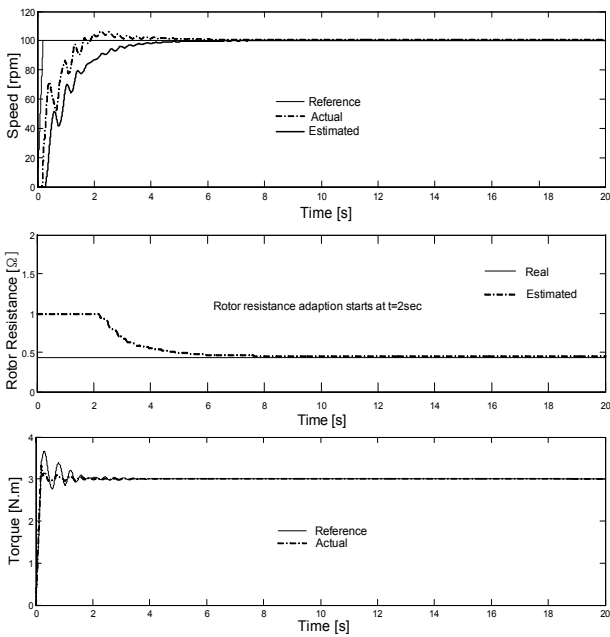
Fig. 7   Rotor resistance identification under constant speed

Fig. 8   Rotor resistance identification under stepwise speed change

Fig. 5 shows the simulation results of the torque response according to stepwise torque commands. It shows a good agreement between torque reference and its responses even though the variable stepwise torque commands are given to the system. We can see some pulses with very small width when the torque command is changed abruptly from phase voltage reference in Fig. 5. It contributes to excellent torque control performance without transient torque. In spite of the voltage command of the sinusoidal wave with pulses, we could not find any spike currents.

Fig. 6 represents the effect of estimation errors of rotor resistance to speed estimation and torque response. The influence on speed estimation is stronger than the one on torque response. It is well known that rotor resistance is a changeable parameter during motor operation. We also know that it is very difficult to estimate rotor resistance simultaneously with speed. In order to estimate speed correctly, we have to identify the rotor resistance in real time.

Fig. 7 shows a sample of simulation results on rotor resistance identification under the condition of constant speed reference. In this simulation, the initial value of the rotor resistance was 1 Ω and a convergence characteristic of rotor resistance according to time t was investigated.
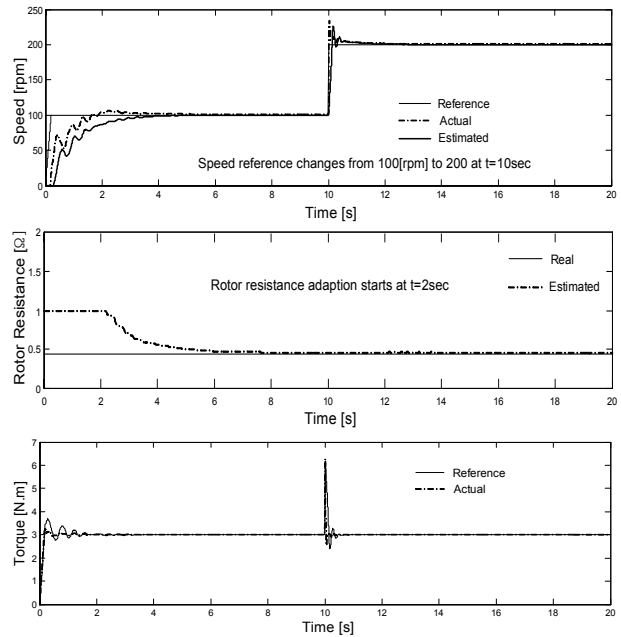
We can see some mismatches between speed reference and estimated speed for a couple of seconds in Fig. 7. This is a result of rotor resistance estimation errors. However, it does not matter because the thermal time constant of rotor resistance is large enough for correct estimation. Moreover, we estimated it from the instant the motor started.

Fig. 8 represents a simulation result for rotor resistance identification under the condition of variable speed reference. We can see that the estimated rotor resistance converges to a real value after a few seconds.
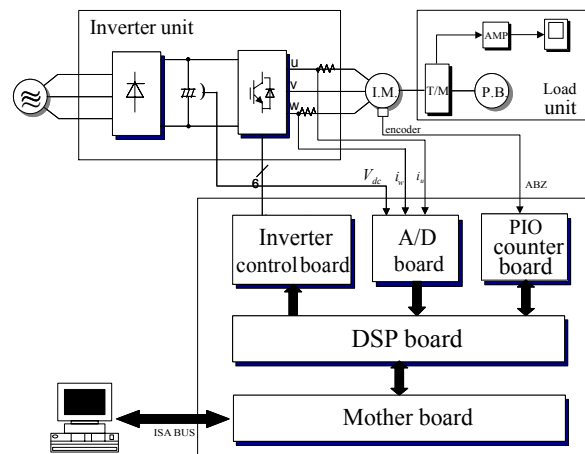

Fig. 9   DSP-based hardware set up for the experiment

4. Experimental Results

Fig. 9 shows the experimental hardware set up based on the DSP system. The dead time of the inverter was 4 μs and the carrier frequency was set at 3 kHz, and the sampling time was 1 ms. Also the A/D converter used to calculate the current had a 12 bits resolution and 3.2 μs conversion time. The rotor flux was given as 0.54 Web during the experiment. The PI gain of the speed controller was set at 0.05 and 0.85 respectively. Also, the PI gain of

the rotor speed estimator was set at 0.0045 and 225. The powder brake (P.B.) system was installed to impose load torque to the I.M.

Fig. 10 represents the experimental results of the estimation of the speed and the rotor resistance simultaneously using the hardware shown in Fig. 9. The motor parameters are shown in Table 1. There are three kinds of speeds in the first graph of Fig. 10, reference speed, actual speed from an encoder, and the estimated speed. The estimated speed shows good agreement with the actual
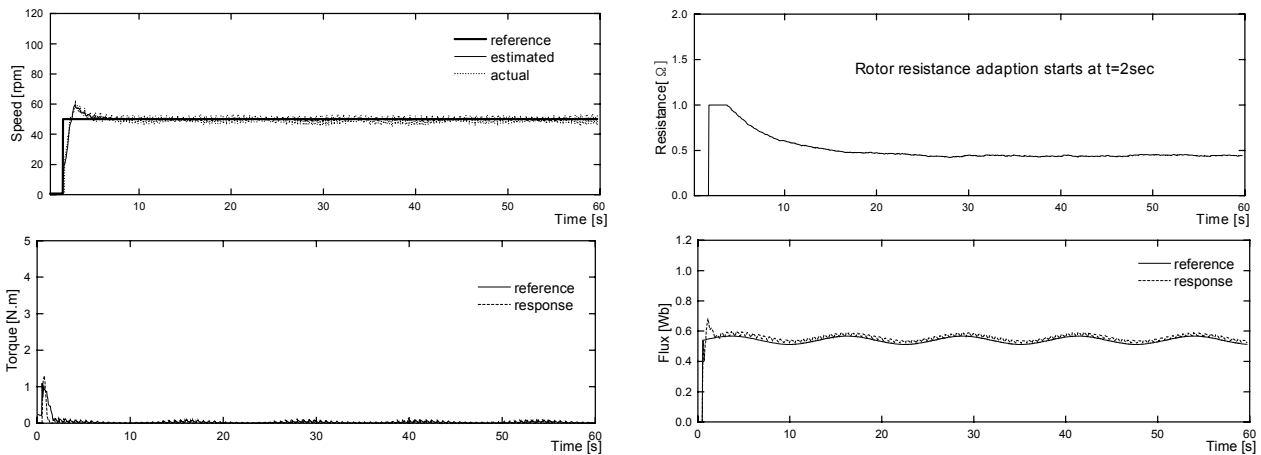

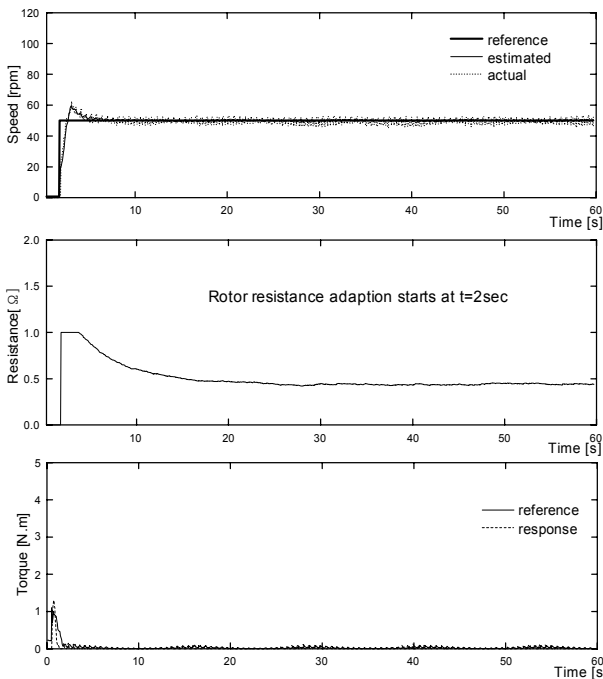Fig. 10 Experimental result of rotor resistance identification under the constant speed

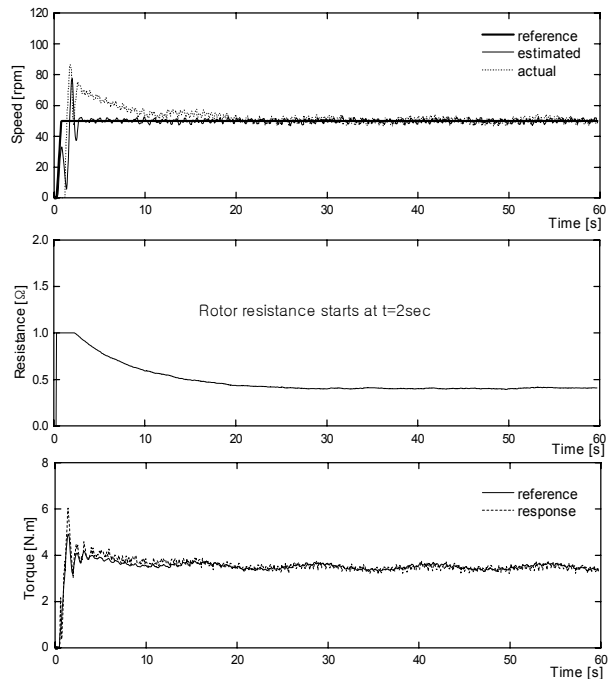Fig. 11 Speed sensorless control at low speed (50 rpm) under no load state

Fig. 12 Speed sensorless control at low speed (50 rpm) under load torque addition

speed. Also, the second graph in Fig. 10 shows estimated rotor resistance using (8). It shows an excellent convergence characteristic from the initial value with some initial errors to the real value after a few seconds. The torque response in the third graph of Fig. 10 was confirmed by the actual torque from toque-meter (T/M) installed on the motor shaft. Also, the response of the rotor flux in the fourth graph of Fig. 10 was calculated from a simplified observer of the Gopinath type [7]. The results showed good agreement between the reference and response.

Fig. 11 and Fig. 12 show the experimental results of the proposed speed sensorless control. The estimated speed coincides with the actual speed even in the state of a load torque addition.

5. Conclusions

This paper proposes the simultaneous estimation of rotor speed and rotor resistance for speed sensorless control of induction motors. In the proposed method, the rotor flux was given a sinusoidal waveform. Using the rotor flux and MRAC, the rotor resistance and the rotor speed could be estimated with fairly good precision. The validity of the proposed speed sensorless control scheme which is robust against rotor resistance variations is confirmed successfully by some numerical simulations and experiments based on the DSP hardware system. Additionally, the proposed rotor resistance estimation can be conducted very simply. Therefore, the proposed system can be accomplished by using cheap microprocessors in various applications.

Acknowledgment

References

[1] S. Suwankawin and S. Sangwongwanich, "A Speed-Sensorless IM Drive With Decoupling Control and Stability Analysis of Speed Estimation", IEEE Trans. Ind. Application, Vol. 49, No. 2, pp. 444-455, 2002.

[2] Y. Kinpara and M. Koyama, "Speed Sensorless Vector Control Method of Induction Motor Including a Low Speed Region", JIEE, Vol. 120D, No. 2, pp. 223-229, 2000.

[3] K. Akatsu and A. Kawamura, "Sensorless Very Low and Zero Speed Estimations with On-Line Secondary Resistance Estimation of Induction Motor Without Adding Any Signal", IEEE Trans. Ind. Applicat, pp. 187-193, 1999.

[4] Jung-Ik Ha and Seung-Ki Sul, "Sensorless Field-Orientation Control of an Induction Machine by High-Frequency Signal Injection", IEEE Transactions on Industy Applications, Vol. 35, No. 1, pp. 45-51, 1999.

[5] Hisao Kubota, Daisuke Yoshihara and Kouki Matsuse, "Rotor- Resistance Adaptation for Sensorless Vector Controlled Induction Machines", T.IEE, Vol. 117-D, No. 8, pp. 940-945, 1997.

[6] Seok-Kwon Jeong, Zhen-Guo Lee and Sam-Sang You, "Sensorless Control of Induction Motors with Simultaneous Estimation of Speed and Rotor Resistance in the Very Low Speed Region", Trans. KIEE, Vol. 53B, No. 9, pp. 552-561, 2004.

[7] B. Gopinath, "On the Control of Linear Multiple Input-Ouput System", The Bell System Technical Journal, 1971.

[8] S. K. Jeong, Z. G. Lee, H. A. Toliyat and P. Niazi, "Sensorless Control of Induction Motors with Simultaneous On-line Estimation of Rotor Resistance and Speed Based on the Feedforward Torque Control Scheme", IEMDC 2003, pp. 1837-1842, 2003.

[9] Z. G. Lee and S. K. Jeong, "Simultaneous Estimation of Rotor Speed and Rotor Resistance of Induction Motor Using Variable Rotor Flux", ICPE 2004, pp. 169-200, 2004.

[10] T. Hayashi, Y. Fuji, and T. Sekiguchi, "Study on an Analytical Solution for Instantaneous Torque Control of an Induction Motor", Annual Conf. of JIEE, Vol. 4, pp. 323-324, 1989.

Zhen-Guo Lee was born in China in 1973. He received his M.S. degree in the Department of Mechatronics Engineering from Pukyong National University, Busan, Korea, in 2001. He completed his Doctoral course in the same department, in 2003. He is interested in the advanced motor control field.

Seok-Kwon Jeong was born in Korea in 1961. He received his M.S. and Engineering Doctorate degrees in the Department of Electrical and Computer Engineering from Yokohama National University, Yokohama, Japan, in 1992 and 1995 respectively. Since 1996, he has been on the faculty of Pukyong National University. He is engaged in research on quick torque control and speed sensorless control of induction machines.